Proceedings of the 35th European Safety and Reliability & the 33rd Society for Risk Analysis Europe Conference
Edited by Eirik Bjorheim Abrahamsen, Terje Aven, Frederic Bouder, Roger Flage, Marja Ylönen
 Published by Research Publishing, Singapore.
doi: 10.3850/978-981-94-3281-3_ESREL-SRA-E2025-P2930-cd

Bayesian Uncertainty Modeling and Risk-Aware Optimization for Unknown Systems

Premjit Saha

Department of Mechanical and Aerospace Engineering, University at Buffalo, USA.
E-mail: premjits@buffalo.edu

Karan Baker

Department of Mechanical and Industrial Engineering, Louisiana State University, USA.
E-mail: kbake54@lsu.edu

Adrian Stein

Department of Mechanical and Industrial Engineering, Louisiana State University, USA.
E-mail: astein@lsu.edu (corresponding author)

This study explores uncertainty classification and modeling, differentiating between aleatory and epistemic uncertainties. Aleatory uncertainty arises from inherent randomness and is commonly represented using random variables, while epistemic uncertainty stems from a lack of precise knowledge about a parameter's true value. Addressing both types is crucial for constructing accurate uncertainty models, which must account for the physical nature of parameters and the available data. The research is motivated by the NASA and DNV 2025 challenge on optimization under uncertainty. To estimate probability densities for both uncertainty types, the study employs Bayesian Inference, which provides a structured approach to updating beliefs about uncertain parameters as new data becomes available. In the design optimization phase, the study utilizes the Shapley value concept to systematically address the subproblems. By fairly evaluating the contribution of each variable before the optimization process, this method enhances resource allocation and decision-making. The derived control inputs are optimized to meet various task-specific objectives, ensuring robust performance.

Keywords: Bayesian Uncertainty Modeling, Uncertainty Quantification, Probability Density Estimation, Shapley Value Theorem, Performance and Reliability-based Design, Stochastic Optimization.

1. Introduction

Uncertainty quantification (UQ) plays a crucial role in engineering and scientific disciplines, particularly when dealing with complex physical systems. Such systems often involve uncertainties arising from inherent randomness (aleatory uncertainty) and limited knowledge about model parameters (epistemic uncertainty). In safety-critical applications, accurately quantifying these uncertainties is essential to ensure reliability and robust performance. However, real-world constraints often limit direct observation of system inputs, making it challenging to characterize their distributions Argell (2025). The framework of the challenge considers a physical system described by an input vector partitioned into aleatory variables ($\mathbf{X}_a$), epistemic variables ($\mathbf{X}_e$), and control variables ($\mathbf{X}_c$). Participants are provided with a computational model capable of generating multivariate time-series responses for specified inputs and random seed parameters. By leveraging both simulated responses from this computational model and limited experimental data from a Simulation Trust Center (STC), participants aim to approximate the unknown distribution of aleatory variables. The ultimate goal is to develop robust methods for uncertainty quantification that generalize effectively across various engineering contexts, enhancing decision-making processes in design optimization under uncertainty Argell (2025). In many engineering and scientific applications, system inputs $\mathbf{X}$ are not directly observable, and we can only access the system response $\mathbf{Y}$ through experiments or simulations. The input space is standardized such that $\mathbf{X} \in [0, 1]^{n_x}$, with $n_x \approx 10$. Given that the true input distribution is

unknown, our goal is to estimate the probability density functions (PDFs) $f_a(\mathbf{X}_a)$ of the aleatory variables $\mathbf{X}_a$ and the tightest intervals for epistemic variables containing their exact (but unknown) values by leveraging observed responses $\mathbf{Y}$.

2. Problem Formulation and Solution

The challenge comprises two distinct but interconnected problems. The first problem focuses on quantifying uncertainty in the input vector $\mathbf{X}$ by integrating simulation outputs from the computational model with experimental data from the physical system. The second problem addresses the optimization of control parameters for the system, explicitly considering uncertainty to achieve a balance between performance and associated risk of failure.

2.1. *Problem 1: Uncertainty Quantification*

Initially, we propose a hierarchical model that captures the conditional relationship between the observed output data and various uncertain parameters, including both aleatory and epistemic uncertainties. To complete the Bayesian specification, we assign informed priors and hyperpriors to these parameters based on available domain knowledge and expert judgment Bozorgzadeh et al. (2023). The hierarchical model aims to capture the uncertainty and variability inherent in both the input vector $\mathbf{X}$ and the system response $\mathbf{Y}$ Sedehi, Hamed and Eftekhar, Saeed and Papadimitriou, Costas (2019). The following is the mathematical formulation of the hierarchical model.

2.1.1. *Model Formulation*

The joint distribution of all variables in the hierarchical model is given as:

$$P(\mathbf{Y}, \boldsymbol{\mu}, \boldsymbol{\Omega}, \boldsymbol{X}_a, \boldsymbol{X}_e) = P(\mathbf{Y} \mid \boldsymbol{\mu}, \boldsymbol{\Omega}) \\ P(\boldsymbol{\mu} \mid \boldsymbol{\mu}_0, \boldsymbol{\Omega}_0) P(\boldsymbol{\Omega} \mid R, \nu) P(\boldsymbol{X}_a) P(\boldsymbol{X}_e), \quad (1)$$

where: $P(\mathbf{Y} \mid \boldsymbol{\mu}, \boldsymbol{\Omega})$: Likelihood of the data. $P(\boldsymbol{\mu} \mid \boldsymbol{\mu}_0, \boldsymbol{\Omega}_0)$: Prior for the mean vector. $P(\boldsymbol{\Omega} \mid R, \nu)$: Prior for the precision matrix. $P(\boldsymbol{X}_a)$: Priors for aleatory uncertainty parameters. $P(\boldsymbol{X}_e)$: Priors for epistemic uncertainty parameters. Data Likelihood: The observed response $\mathbf{Y}_i = [y_1 \ y_2 \ y_3 \ \dots \ y_6]^T$ for each observation i follows a multivariate normal distribution: $\mathbf{Y}_i \sim \mathcal{N}(\boldsymbol{\mu}, \boldsymbol{\Omega}^{-1})$, where $\boldsymbol{\mu}$ is the mean vector and $\boldsymbol{\Omega}$ is the precision matrix (inverse of the covariance matrix) Hoff (2009). Prior for Mean Vector: The mean vector $\boldsymbol{\mu}$ is modeled as a multivariate normal distribution: $\boldsymbol{\mu} \sim \mathcal{N}(\boldsymbol{\mu}_0, \boldsymbol{\Omega}^{-1})$, $\boldsymbol{\mu} \in \mathbb{R}^{6\times 1}$ where $\boldsymbol{\mu}_0$ is the prior mean and $\boldsymbol{\mu}_0 = \overline{\mathbf{Y}}$, where $\overline{\mathbf{Y}} = \sum_{i=1}^{K} \mathbf{Y}_i / K$. Prior for Precision Matrix: The precision matrix $\boldsymbol{\Omega}$ follows a Wishart distribution Koop and Korobilis (2010), Uhlig (1994): $\boldsymbol{\Omega} \sim \mathcal{W}(\mathbf{R}, \nu)$, where $\mathbf{R}$ is called the scale matrix and ν is the degrees of freedom. This choice ensures that the precision matrix remains positive definite. Covariance Matrix: The covariance matrix $\boldsymbol{\Sigma}$ is defined as the inverse of the precision matrix: $\boldsymbol{\Sigma} = \boldsymbol{\Omega}^{-1}$, both $\boldsymbol{\Omega}, \boldsymbol{\Sigma} \in \mathbb{R}^{6\times 6}$.

2.1.2. *Aleatory Uncertainty*

Aleatory uncertainty is captured using beta distributions Stafford (2020) for parameters $X_{a,1}$ and $X_{a,2}$, which represent probabilities:

$$X_{a,1} \sim \text{Beta}(\alpha_1, \beta_1) \quad (2a)$$
$$a_1 \sim U(0,1), \quad \alpha_1 = 1/a_1 \quad (2b)$$
$$b_1 \sim U(0,1), \quad \beta_1 = 1/b_1. \quad (2c)$$

Similarly, for X_{a2}:

$$X_{a,2} \sim \text{Beta}(\alpha_2, \beta_2) \quad (3a)$$
$$a_2 \sim U(0,1), \ \alpha_2 = 1/a_2 \quad (3b)$$
$$b_2 \sim U(0,1), \ \beta_2 = 1/b_2. \quad (3c)$$

2.1.3. *Epistemic Uncertainty*

Epistemic uncertainty is modeled using normal distributions for parameters $X_{e,1}$, $X_{e,2}$, and $X_{e,3}$:

$$X_{e,1} \sim N(\mu_{e_1}, 1/\sigma_{e_1}) \quad (4a)$$
$$\mu_{e_1} \sim U(0,1), \ \sigma_{e_1} \sim \Gamma(a_0, b_0). \quad (4b)$$

Similarly, for $X_{e,2}$:

$$X_{e,2} \sim N(\mu_{e_2}, 1/\sigma_{e_2}) \quad (5a)$$
$$\mu_{e_2} \sim U(0,1), \ \sigma_{e_2} \sim \Gamma(a_0, b_0). \quad (5b)$$

and $X_{e,3}$:

$$X_{e,3} \sim N(\mu_{e_3}, 1/\sigma_{e_3}) \quad (6a)$$
$$\mu_{e_3} \sim U(0,1), \ \sigma_{e_3} \sim \Gamma(a_0, b_0). \quad (6b)$$

The distributions Beta$(\cdot,\cdot)$, $U(\cdot,\cdot)$, and $\Gamma(\cdot,\cdot)$ represent the Beta, Uniform, and Gamma distributions, respectively. Here, α and β are the shape parameters of the Beta distribution; $U(a,b)$ denotes a Uniform distribution with lower and upper bounds a and b, respectively; and a_0 and b_0 are the shape and rate parameters of the Gamma distribution.

2.1.4. *Insights and Motivation for the Hierarchical Model*

We selected the multivariate normal distribution for two key reasons: When numerous small, independent effects combine, their aggregate tends toward a normal distribution. This property extends to the multivariate case via the central limit theorem, making the normal assumption natural for complex systems with additive uncertainties. Given constraints on mean $\boldsymbol{\mu}$ and covariance $\boldsymbol{\Sigma}$, the multivariate normal distribution maximizes entropy. This makes it the least biased choice when only these moments are known, avoiding unwarranted assumptions about higher-order structure Uhlig (1994). Since each epistemic parameter has an underlying true value within the interval $[0,1]$, our objective is to construct a prior distribution that is highly concentrated around this value. Effectively, we aim for the prior to resemble a Gaussian distribution with an extremely small variance—approaching an impulse function with a very narrow base. By choosing identical shape parameters ($a_0 = 10^{-1}$) and rate parameters ($b_0 = 10$), which are necessary for defining a Gamma distribution for each epistemic parameter, we uniformly control the variance across all of them. As long as the variance of each epistemic parameter remains small, we are satisfied with the model. We found no need to introduce additional uncertainty or an extra hierarchical layer that would unnecessarily complicate the system. Finally, we have chosen the Beta distribution for aleatory parameters since it is bounded within the interval $X_a \in [0,1]$. We ensure that the Beta distribution remains bounded by choosing both shape parameters, α and β, such that $\alpha \geq 1$ and $\beta \geq 1$.

2.1.5. *Summary of the $\mathbf{X}_c$ Sample Points*

Next, the observed output dataset derived from both the true system and computational model will be utilized to construct the uncertainty model, referred to as UM1 Argell (2025). The control variables $\mathbf{X}_c$ are defined within a three-dimensional unit cube, i.e., $\mathbf{X}_c \in [0,1]^3$. Due to computational constraints, only 10 sample points for $\mathbf{X}_c$ are selected. These points are chosen along two distinct straight lines within the unit cube, each defined by parametric equations as follows:

$$\text{Line 1: } [x,y,z] = [t,t,t],\ t \in [0,1] \tag{7a}$$

$$\text{Line 2: } [x,y,z] = [1-t,t,t],\ t \in [0,1] \tag{7b}$$

Table 1.: Points for $\mathbf{X}_c$ from STC simulation.

t	$\mathbf{X}_c(x,y,z)_{\text{Line 1}}$	$\mathbf{X}_c(x,y,z)_{\text{Line 2}}$
0	[0.00, 0.00, 0.00]	[1.00, 0.00, 0.00]
0.25	[0.25, 0.25, 0.25]	[0.75, 0.25, 0.25]
0.50	[0.50, 0.50, 0.50]	[0.50, 0.50, 0.50]
0.75	[0.75, 0.75, 0.75]	[0.25, 0.75, 0.75]
1	[1.00, 1.00, 1.00]	[0.00, 1.00, 1.00]

Diagonal sampling is advantageous under strict computational budgets (e.g., 10 samples) due to its deterministic nature, reproducibility, and explicit targeting of extreme hypercube corners. However, it lacks uniform dimensional coverage. When resources permit, Latin Hypercube Sampling remains a better choice for comprehensive multi-dimensional modeling.

2.1.6. *Results*

The multidimensional time series output data was generated both locally through simulation and remotely from STC. Initially, for each baseline set of control parameters (Table 1), we generated 100 i.i.d. multivariate time series datasets from STC. Each dataset comprises 6 outputs sampled at 60 temporal points across $t \in [0,1]$. These datasets, derived from specific $\mathbf{X}_c$ parameter values, were then used to construct a hierarchical Bayesian model following the `rjags` R package methodology. The Markov Chain Monte Carlo (MCMC) procedure is employed to robustly explore the posterior distribution of both aleatory and epistemic parameters. Each chain undergoes a burn-in phase consisting of $2,000$ iterations, ensuring

convergence to the target posterior distribution. Subsequently, posterior sampling is performed for $10,000$ iterations per chain using statistical packages available in R. Each MCMC chain, generated from data derived from STC for a selected baseline $\mathbf{X}_c$, demonstrates strong convergence diagnostics after burn-in, particularly according to the method developed by Adrian Raftery and Steven Lewis Gottardo and Raftery (2008),Gilks et al. (1998). Subsequently, a set of 10 MCMC chains is constructed for each aleatory and epistemic parameter, and their corresponding posterior PDFs are estimated. Table 2 contains statistical summaries for each aleatory and epistemic parameter.

Table 2.: Statistical summary of posterior PDFs for uncertain parameters.

parameters	mean	standard deviation	Quantile values 2.5%	97.5%
$X_{a,1}$	0.496705	0.303231	0.01665	0.98223
$X_{a,2}$	0.497828	0.304109	0.01688	0.98430
$X_{e,1}$	0.515389	0.102518	0.3486	0.6818
$X_{e,2}$	0.52714	0.10099	0.3637	0.6927
$X_{e,3}$	0.52460	0.11704	0.3348	0.7138

Fig. 1 displays the posterior PDFs obtained from the stationary distributions of multiple MCMC chains corresponding to each uncertain parameter and it also illustrates a significant reduction in the width of the support for all three epistemic parameters compared to the initial support set provided. This reduction results in a narrow interval, represented as a PDF, which provides a more precise estimate of the unknown true values for each of these parameters. Fig. 2 displays the posterior PDFs derived from stationary distributions of MCMC chains, generated during the Uncertainty Quantification Model 2 (UM2) calibration process. These PDFs were computed using the highest-density 95% subset of the data, a statistically robust approach that prioritizes the most informative observations. This methodology constitutes a key deliverable of subproblem 1.2, as formally defined in Argell (2025). Moreover, Table 3 provides quantitative counterparts through statistical summaries for both $\mathbf{X}_a$ and $\mathbf{X}_e$ parameters under this constrained data regime. Subproblem 1.2 requires minor adjustments in the hierarchical model for both aleatory and epistemic parameters. For instance, the revised distribution for $X_{a,1}$ becomes:

$$X_{a,1} = z_l + (z_u - z_l)z, \;\; z \sim \text{Beta}(\alpha_1, \beta_1) \tag{8a}$$
$$a_1 \sim U(0,1), \quad \alpha_1 = 1/a_1 \tag{8b}$$
$$b_1 \sim U(0,1), \quad \beta_1 = 1/b_1. \tag{8c}$$

Here, z_l and z_u denote the lower and upper bounds (2.5% and 97.5% quantiles from Table 2) constraining $X_{a,1}$. Analogous modifications apply to $X_{a,2}$. For epistemic parameters, $X_{e,1}$ is redefined as:

$$X_{e,1} \sim N(\mu_{e_1}, 1/\sigma_{e_1}) \tag{9a}$$
$$\mu_{e_1} \sim U(m_0, n_0),\ \sigma_{e_1} \sim \Gamma(a_0, b_0). \tag{9b}$$

with m_0 and n_0 similarly derived from Table 2. Identical adjustments apply to $X_{e,2}$ and $X_{e,3}$.

Table 4 summarizes the estimated prediction interval bounds g_1 (minimum acceptable bound) and g_2 (maximum tolerable limit) for each output state, computed across the full parameter space of the $\mathbf{X}_c$ dataset. Here, α represents the chosen confidence level, and $y_1, y_2, y_3 \ldots y_6$ denote the output variables conditioned on $\mathbf{X}_c$ parameters. These bounds are formally defined as $g_1 = \inf\{f_1\}$ and $g_2 = \sup\{f_2\}$, which are

$$f_1 = u \mid \max_{\mathbf{X}_e \in E} p_u(\mathbf{X}_e, \mathbf{X}_c, u) \leq 1 - \alpha \tag{10a}$$
$$f_2 = l \mid \max_{\mathbf{X}_e \in E} p_l(\mathbf{X}_e, \mathbf{X}_c, l) \leq 1 - \alpha. \tag{10b}$$

The numerical framework for subproblem 1.3 was constructed through multivariate interpolation across a structured parameter grid, with distinct resolutions for the $\mathbf{X}_a$ and $\mathbf{X}_e$ parameters. Our Shapley value analysis (detailed in Section 2.2) revealed significantly lower sensitivity to epistemic parameters compared to aleatory parameters, justifying an asymmetric grid configuration: a refined 7×7 Chebyshev grid for aleatory parameters was paired with a coarser $3 \times 3 \times 3$ epistemic grid. This design choice reflects the relative parameter influence while maintaining computational efficiency. Chebyshev nodes were employed for both parameter classes to minimize Runge's phenomenon in multidimensional

interpolation. Splines were then applied to construct continuous response surfaces over the grid. At each epistemic grid node, we computed the boundary probabilities in Eqn. (10) where,

$$p_u(\mathbf{X}_e, \mathbf{X}_c, u) = \mathbb{P}\left(\max_{0\le t\le 1} y(\mathbf{X}, s, t) > u\right) \tag{11a}$$

$$p_l(\mathbf{X}_e, \mathbf{X}_c, l) = \mathbb{P}\left(\min_{0\le t\le 1} y(\mathbf{X}, s, t) < l\right), \tag{11b}$$

following the methodology from Argell (2025), where $\mathbf{X} = [\mathbf{X}_a, \mathbf{X}_e, \mathbf{X}_c]$. Final estimates of g_1 and g_2 were determined through extremal value aggregation across all epistemic parameter configurations for fixed $\mathbf{X}_c$ settings.

Table 3.: Statistical summary of posterior PDFs for uncertain parameters by using the "most informative" 95% of the data.

parameters	mean	standard deviation	Quantile values 2.5%	97.5%
$X_{a,1}$	0.502746	0.293117	0.03613	0.96711
$X_{a,2}$	0.503434	0.291773	0.03268	0.96907
$X_{e,1}$	0.5609452	0.0452712	0.4818	0.6340
$X_{e,2}$	0.6000211	0.0514455	0.5083	0.6906
$X_{e,3}$	0.608562	0.047600	0.5282	0.6933

Table 4.: Prediction intervals for α = 0.999, 0.95

Variables	$\alpha = 99.9\%$		$\alpha = 95\%$	
	g_1	g_2	g_1	g_2
y_1	0	3.35	0.0056	3, 35
y_2	0	3.35	0	3.35
y_3	0	3.35	0.0056	3, 35
y_4	0	8397.3	0.7688	6834.2
y_5	0	3452.0	0.2918	2551.5
y_6	0	2990.4	0.2715	2406.6

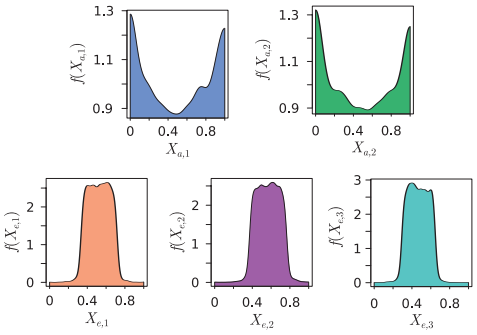

Fig. 1.: Posterior PDFs from MCMC simulation for $\mathbf{X}_a$ and $\mathbf{X}_e$ from UM1.

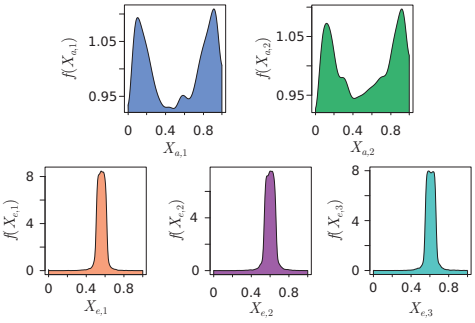

Fig. 2.: Posterior PDFs from MCMC simulation for $\mathbf{X}_a$ and $\mathbf{X}_e$ by using the "most informative" 95% of the data (UM2).

2.2. *Problem 2: Design Optimization*

2.2.1. *Shapley Value Theorem*

The definition of Shapley effects for a model with d uncertain variables is given by Iooss and Prieur (2017):

$$Sh_\gamma = \frac{1}{d}\sum_{v\subseteq -\{\gamma\}} \binom{d-1}{|v|}^{-1} \left(w(v\cup\{\gamma\}) - w(v)\right), \tag{12}$$

where $w(...)$ represents the worth or value of the coalition, and $-\{\gamma\}$ denotes the set of indices $1, ..., d$ excluding γ. $w(v \cup \{\gamma\})$ is a coalition including variable γ and $w(v)$ excluding variable γ. The marginal contribution of variable γ to a coalition v is referred to as Shapley effects. We define the worth of a coalition for systems where the players are characterized probabilistically as Iooss and Prieur (2017):

$$w(v) = \frac{Var\left(\mathbb{E}[Z|\mathcal{X}_v]\right)}{Var(Z)}, \tag{13}$$

where $\mathcal{X} = (\mathcal{X}_1, ..., \mathcal{X}_d)$ is a set of continuous independent variables. $\mathcal{X}_v$ denotes the set of inputs indexed by $v(v \subseteq 1, ..., d)$. Z is the model response with $Z \in \mathbb{R}$. Then, the Shapley value concept has the following features:

- Of relevance when contribution of each player is unequal
- Cooperation among players is beneficial rather than working independently
- Shapley effects are non-negative

- The sum of all Shapley effects is 1

In the NASA-UQ challenge the following cost function is considered:

$$J(\mathbf{X}_e, \mathbf{X}_c) = \int_0^1 \sum_{i \in I_1} \mathbb{E}\left[y_i(\mathbf{X}_a, \mathbf{X}_e, \mathbf{X}_c, s, t)\right] dt \quad (14)$$

where $\mathbb{E}[\cdot]$ is the expected value operator with respect to $\mathbf{X}_a$ and s. The set of I_1 represents the outputs y_1, y_2, and y_3. In this work UQLab Marelli et al. (2015) is used as a tool for the sensitivity analysis. 8000 MC samples are used to compute all order Sobol indices. Since we have 6 uncertain parameters $[X_{e,1}, X_{e,2}, X_{e,3}X_{c,1}, X_{c,2}, X_{c,3}]$ we have to compute up to a 6th order Sobol index. For the computation an Intel(R) Core(TM) i7-14700F CPU, 2.10GHz, 20 Cores with 32GB RAM is utilized. Song et al. Song et al. (2016), established the connection between the first-order, total, and Shapley effects using the concept of semivalues. Furthermore, this work uses the mapping between all order the Sobol indices to Shapley effects as presented in Stein and Singh (2023). For UQLab the control variables are assumed to be uniformly distributed between 0 and 1 while the epistemic variables are assumed to be normal distributed with a mean and standard deviation as presented in Table 2. $X_{a,1}$ and $X_{a,2}$ are calculated from 4 Legendre-Gauss Quadrature points for the interval from 0 to 1 making it 16 different nodes. The output for the sensitivity study is the cost J from Eqn. (14). Fig. 3 illustrates that the epistemic variables have a minor influence on the cost J. If any epistemic variable has an influence it is $X_{e,1}$ with a Shapley Effect of 0.011. The most influential variables are in the order of $X_{c,1}$, $X_{c,2}$, and $X_{c,3}$, with Shapley effects of 0.5056, 0.2523, and 0.2253, respectively. Again the Shapley effects all sum up to unity, which provides a graspable metric to quantify the uncertainty of this complex system. For illustrating the range of the objective function J and the range of failure probability pof_{sys} we used 10 datasamples from our PDFs of $\mathbf{X}_e$.

2.2.2. *Finding $\mathbf{X}_c$ for Performance-based Design*

We assume that the PDFs of $\mathbf{X}_e$ are identified as described in section 2.1.6. The PDFs of $\mathbf{X}_a$ can not be represented with any standard PDF. Therefore, the expected value of $\mathbf{X}_a$ is calculated with the Legendre-Gauss quadrature points, where the order is chosen to be 4. The respective Legendre-Gauss quadrature weights are taken into account. This and the following grid-search process to initialize the optimization are presented in Fig. 4. The control variables are defined over an interval from 0 to 1. The optimization problem in this section is based on running an outer optimization loop for $\mathbf{X}_c$ and an inner optimization loop for $\mathbf{X}_e$. The procedure from section 2.2.1 revealed that the control variables are most influential on the cost J. Instead of brute force optimizing over the whole space, we split $\mathbf{X}_c$ up into 0.2 increments to perform a grid search and sample 10 different sets for $\mathbf{X}_e$ using the MATLAB command "datasample". This leads to 1250 samples which are simulated for the grid-based search. The set that leads to the optimal $\max_{\mathbf{X}_e \in E} \min J(\mathbf{X}_e, \mathbf{X}_c)$, is used as an initial guess for the double optimization problem, which in our case $\mathbf{X}_c = [0.4,\ 0.8,\ 0.8]$ (see Fig. 4). The solver used for this optimization is SQP. The $\mathbf{X}_c^* = [0.5000,\ 0.8477,\ 0.7590]$ with an $\mathbf{X}_e^* = [0.3368,\ 0.4437,\ 0.6276]$. The cost for these parameters is $J = 8.2130$. The range of J and pof_{sys} over X_e for $\mathbf{X}_c^*$ is $[8.2086, 8.2295]$ and $[0.2284, 0.2596]$, respectively.

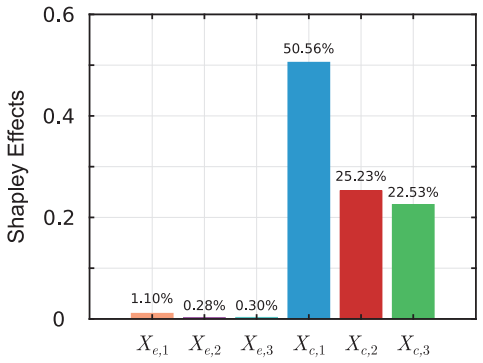

Fig. 3.: Shapley Effects of $\mathbf{X}_e$ and $\mathbf{X}_c$ for set I_1.

2.2.3. *Finding $\mathbf{X}_c$ for Reliability-based Design*

For the responses in I_2 (referring to the states y_4, y_5, and y_6), the limit state functions are defined

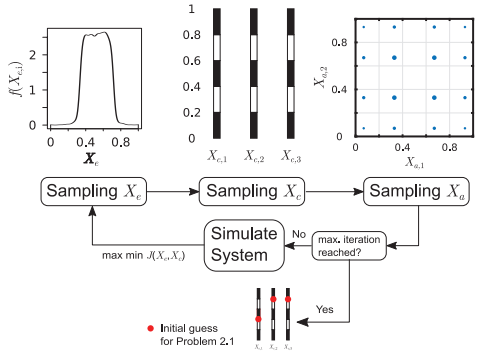

Fig. 4.: Grid Search for Initial Guess for Performance-based Design.

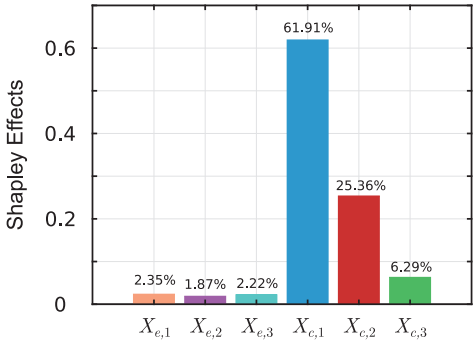

Fig. 5.: Shapley Effects of $\mathbf{X}_e$ and $\mathbf{X}_c$ for set I_2.

as:

$$g_i(\mathbf{X}, s) = c_i - \max_{0 \le t \le 1} |y_i(\mathbf{X}, s, t)|, \quad \forall i \in I_2, \quad (15)$$

where the constants c_i are $[2750, 2000, 1000]$. The event $g_i(\mathbf{X}, s) < 0$ represents a failure in the i-th physical response. This implies that y_i exceeded at a certain time instant the constant value of c_i. The individual failure probability is defined as:

$$\text{pof}_i(\mathbf{X}_e, \mathbf{X}_c) = \mathbb{P}[g_i(\mathbf{X}_a, \mathbf{X}_e, \mathbf{X}_c, s) < 0], \quad (16)$$

where $\mathbb{P}[\cdot]$ is the probability with respect to $\mathbf{X}_a$ and s. The system probability of failure is:

$$\text{pof}_{\text{sys}}(\mathbf{X}_e, \mathbf{X}_c) = \mathbb{P}\big[\min_{i \in I_2} g_i(\mathbf{X}_a, \mathbf{X}_e, \mathbf{X}_c, s) < 0\big]. \quad (17)$$

For comparison to the performance-based design we choose the cost J as an output for the Shapley effect analysis. Fig. 5 illustrates that the epistemic variables have a minor influence on the cost J. The most influential variables are in the order of $X_{c,1}$, $X_{c,2}$, and $X_{c,3}$, with Shapley effects of 0.6191, 0.2536, and 0.0629, respectively. Again the Shapley effects all sum up to unity. Here a grid-search method is used to get a general idea of which $\mathbf{X}_c$ is being used as an initial guess for the optimizer. Since the set of outputs in I_2 depend more on $X_{c,1}$ (see Fig. 5) we perform a grid search of $10 \times 6 \times 6$ as illustrated in Fig. 4. $\mathbf{X}_a$ is calculated with the Legendre-Gauss quadrature points by a 6×6 grid. From the findings of the grid-search we initialize our system with the variable $\mathbf{X}_c = [0.4, 0.6, 0.95]$. To calculate pof_{sys} we interpolate the time-series data for the set I_2 with 100 interpolation points linearly. To blend in the uncertainty of epistemic variables we sample $\mathbf{X}_e$ in each optimization loop. Fig. 6 illustrates the optimization process for subproblem 2.2 and 2.3. $\mathbf{I}_1$ and $\mathbf{I}_2$ represent all sets of I_1 and I_2. For the reliability-based design $\mathbf{X}_c^* = [0.419152706, 0.562926273, 0.984253589]$ with a final objective convergence of $\text{pof}_{\text{sys}} = 0.0003415$.

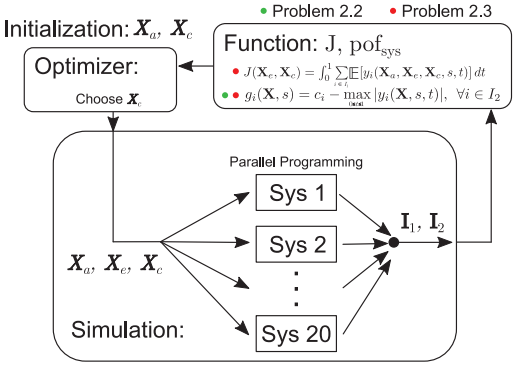

Fig. 6.: Schematic Overview of Optimization in Problem 2.2 and 2.3.

The range of J and pof_{sys} over X_e for $\mathbf{X}_c^*$ is $[7.6232, 7.7637]$ and $[0.0003415, 0.0573048]$, respectively.

2.2.4. *Finding $\mathbf{X_c}$ for ϵ-based Design*

Subproblem 2.3 is the combination of subproblems 2.1 and 2.2, except that 2.2 is treated as a constraint. This attempts to maximize

the cost function in Eqn. (14) while not allowing the probability of failure of the system to exceed a certain threshold denoted as ϵ, which is given as either $\epsilon_1 = 10^{-3}$ and $\epsilon_2 = 10^{-4}$. As an initial $\mathbf{X}_c$ for subproblem 2.3, we use the converged solution $\mathbf{X}_c^*$ from subproblem 2.2. For ϵ_1 we derived $\mathbf{X}_{c,\epsilon_1}^* = [0.421990665,\ 0.566337066,\ 0.985701343]$. The range of J and pof_{sys} over X_e for $\mathbf{X}_c^*$ is $[7.6104, 7.6501]$ and $[0.000310, 0.001000]$, respectively. For ϵ_2 we derived $\mathbf{X}_{c,\epsilon_2}^* = [0.423591229,\ 0.568260698,\ 0.986517853]$. The range of J and pof_{sys} over X_e for $\mathbf{X}_c^*$ is $[7.5798, 7.5948]$ and $[0.000068, 0.000100]$, respectively.

3. Conclusion

In safety-critical applications, a reliability-based design framework should be used. This study employed Legendre-Gauss quadrature for sampling the design variables $\mathbf{X}_a$, prioritizing accurate estimation of the expected value for the objective function J. Although alternative sampling strategies such as direct sampling from the probability density function or Latin Hypercube Sampling could have improved the accuracy of pof_{sys}, they were less effective in capturing the expected objective. Given additional computational resources, increasing the number of quadrature points would be a promising approach to enhance numerical accuracy. Our findings indicate that Problem 1 already imposed significant computational demands, with Problem 2 requiring substantially more effort. The application of the Shapley value theorem was instrumental in guiding efficient allocation of computational resources. The observed underestimation of required computational effort underscores the need for more efficient numerical strategies or access to greater computational capacity in future studies. Moreover, future work may explore the integration of artificial intelligence to better understand the complex system dynamics. Lastly, we observed that the choice of the initial guess for $\mathbf{X}_c$ has a considerable impact on the convergence behavior toward the optimal solution $\mathbf{X}_c^*$.

References

Argell, C. (2025). The nasa and dnv challenge on optimization under uncertainty 10.01.

Bozorgzadeh, N., Z. Liu, F. Nadim, and S. Lacasse (2023). Model calibration: A hierarchical bayesian approach. *Probabilistic Engineering Mechanics 71*(6), 103379.

Gilks, W. R., S. Richardson, and D. J. Spiegelhalter (1998). *Markov chain Monte Carlo in practice*. Boca Raton Fla.: Chapman & Hall.

Gottardo, R. and A. E. Raftery (2008). Markov chain monte carlo with mixtures of mutually singular distributions. *Journal of Computational and Graphical Statistics 17*(4), 949–975.

Hoff, P. D. (2009). *A First Course in Bayesian Statistical Methods*. New York, NY: Springer New York.

Iooss, B. and C. Prieur (2017). Shapley effects for sensitivity analysis with correlated inputs: Comparisons with sobol' indices, numerical estimation and applications. *International Journal for Uncertainty Quantification*.

Koop, G. and D. Korobilis (2010). *Bayesian multivariate time series methods for empirical macroeconomics*. Boston: Now.

Marelli, S., C. Lamas, and B. Sudret (2015). Uqlab user manual – sensitivity analysis.

Sedehi, Hamed and Eftekhar, Saeed and Papadimitriou, Costas (2019). Quantification of aleatory uncertainty in modal updating problems using a new hierarchical bayesian framework. *University of Thessaly Institutional Repository*.

Song, E., B. L. Nelson, and J. Staum (2016). Shapley effects for global sensitivity analysis: Theory and computation. *SIAM/ASA Journal on Uncertainty Quantification 4*(1), 1060–1083.

Stafford, R. D. (2020). *Analysis of Beta Distribution for Subjective Uncertainty Analysis in Cost Models*. Masters, Air Force Institute of Technology.

Stein, A. and T. Singh (2023). Shapley effect estimation using polynomial chaos.

Uhlig, H. (1994). On singular wishart and singular multivariate beta distributions. *The Annals of Statistics 22*(1).